Korea-Australia Rheology Journal
Vol. 21, No. 1, March 2009 pp. 39-46

Fluid-structure interactions of physiological flow in stenosed artery

Bahtiyor Buriev[1], Taedong Kim[2] and Taewon Seo[1,*]
[1]*School of Mechanical Engineering, Andong National University, Andong, 760-749, Korea*
[2]*Deptment of Environmental Engineering, Andong National University, Andong, 760-749, Korea*
(Received August 24, 2008; final revision received December 10, 2008)

Abstract

Atherosclerosis is a disease that narrows, thickens, hardens, and restructures a blood vessel due to substantial plaque deposit. The geometric models of the considered stenotic blood flow are three different types of constriction of cross-sectional area of blood vessel; 25%, 50%, and 75% of constriction. The computational model with the fluid-structure interaction is introduced to investigate the wall shear stresses, blood flow field and recirculation zone in the stenotic vessels. The velocity profile in a compliant stenotic artery with various constrictions is subjected to prescribed physiologic waveform. The computational simulations were performed, in which the physiological flow through a compliant axisymmetric stenotic blood vessel was solved using commercial software ADINA 8.4 developed by finite element method. We demonstrated comparisons of the wall shear stress with or without the fluid-structure interaction and their velocity profiles under the physiological flow condition in the compliant stenotic artery. The present results enhance our understanding of the hemodynamic characteristics in a compliant stenotic artery.

Keywords : stenosis, atherosclerosis, recirculation zone, fluid-structure interaction, physiological flow

1. Introduction

Atherosclerosis tends to develop in preferred sites, such as the bifurcations and flow divisions of the arteries (Karino *et al.*, 1988). The development and progression of the atherosclerosis are related to the complex flow field occurring in the inner wall of curvatures and bifurcations of the arteries. It is widely known that there is the correlation between atherosclerosis lesion location and low or oscillating wall shear stress (Karino *et al.*, 1988; Ku *et al.*, 1985).

Many cardiovascular diseases are closely associated with the flow conditions in the blood vessel. One major type of arterial disease is atherosclerosis which is characterized by localized accumulation of cholesterol and lipid substances. It is commonly referred to as a "hardening" of the arteries. It is caused by the formation of multiple plaques within the arteries.

The symptom of atherosclerotic cardiovascular disease is heart attack or sudden cardiac death. The most artery flow disrupting events occur at locations with less than 50% of lumen narrowing (~20% stenosis is average) (Glagov *et al.*, 1987). According to cardiac stress testing, traditionally the most commonly performed non-invasive testing method for blood flow limitations generally only detects lumen narrowing of ~75% or greater.

From clinical trials, 20% is the average stenosis at plaques that subsequently rupture with resulting complete artery closure (Glagov *et al.*, 1987). Most severe clinical events do not occur at plaques that produce high-grade stenosis. Only 14% of heart attacks occur from artery closure at plaques producing 75% or greater stenosis prior to the vessel closing.

In Wikipedia the definition of fluid-structure interaction (FSI) is "FSI occurs when a fluid interacts with the solid structure, exerting pressure on it which may cause deformation in the structure and thus alter the flow of fluid itself". A fully coupled fluid-structure interaction means that the response of the solid is strongly affected by the response of the fluid, and vice versa. Thus, basic understanding of fluid-structure interaction model is essential in cardiovascular system.

Recent development in the blood flow simulation due to the computer development is the numerical simulation of fluid-structure interaction (FSI) between a blood flow and stenosed arteries. Tang *et al.* (2001a) considered FSI for unsteady viscous flow in elastic stenotic tubes simulating blood flow in stenotic carotid arteries. They observed complex flow patterns and high shear stresses at the throat of the stenosis in case of compressive stresses inside the tube. Yamaguchi *et al.* (1998) considered FSI in the collapse and ablation of atheromatous plaque in coronary arteries and found that wall shear stress distribution has localized pattern and that the dragging force from fluid has a consid-

*Corresponding author: dongjin@andong.ac.kr

erable effect on wall compression under physiological conditions. Powell (1991) measured the tube law for bovine carotid artery and studied the effects of severity of stenosis. Their results showed that the tube wall collapsed under physiological conditions. Buchanan *et al.* (2000) studied rheological effects on pulsatile laminar flow through an axisymmetric stenosed tube and found that they could affect wall shear stress quantities.

An FSI model becomes essential to achieve a basic understanding of effects of various mechanical forces involved in arterial disease development. The present study is concerned with physiological flow both in elastic and rigid wall vessels with 25, 50 and 75% constriction of cross-sectional area in stenosed arteries. The objective of this study is to understand how the flow features and wall shear stress field change with the development of stenosis by numerically analyzing the interactions between a blood flow and a stenosed wall. In the present study, we investigate shear stresses along the wall, velocity field, wall motion and recirculation zones in the different type of constriction of the blood vessel.

2. Formulation of the problem

2.1. Geometric model of blood vessel

The diseased artery was modeled as an axisymmetric stenosis with 25%, 50% and 75% area reductions as shown in Fig. 1, respectively. Two cases were studied here: physiological flow model with rigid wall assumption (No FSI model in Fig. 1 (a)), and physiological flow with an elastic wall (FSI model in Fig. 1 (b)). The No FSI model is built without incorporating the fluid-structure interaction while the FSI model is considered with incorporating the fluid-wall interaction. As shown in Fig. 1, the total length of the geometry of a cylindrical tube adopted is 24*D*, where D=4 *mm* is the diameter of the non-stenosed region of the artery. Entrance length of the blood flow to stenosis region is 2*D*. t_1, t_2, t_3 are assumed stenotic rates in No FSI and FSI models, respectively. The length of the stenosis is 2*D*. Thickness (t_h) of the blood vessel wall is assumed to be *D*/4.

2.2. Flow modeling

The blood is assumed to be incompressible, laminar and Newtonian fluid, while the blood vessel wall is isotropic and elastic. The properties of blood are assumed to have density ρ_f=1060 *kg/m*^{3} and a dynamic viscosity μ=0.0035 *kg/m·s*.

The governing equations for the fluid domain are given as follows:

· Continuity equation

$$\frac{\partial u_i}{\partial x_i} = 0 \tag{1}$$

· Momentum equations

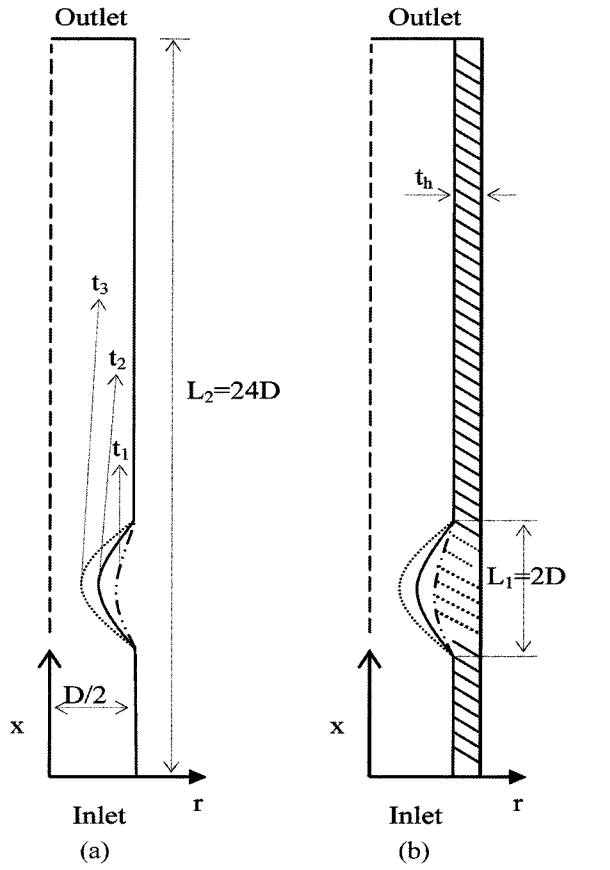

Fig. 1. Schematic geometries of the stenosed blood vessel (a) with rigid wall model (No FSI Model), (b) with elastic wall model (FSI Model).

$$\frac{\partial u_i}{\partial t} + (u_j - \widehat{u}_j)\frac{\partial u_i}{\partial x_j} = \frac{1}{\rho_f}\frac{\partial p}{\partial x_j} + \frac{\mu}{\rho_f}\frac{\partial^2 u_i}{\partial x_j^2} \tag{2}$$

where subscripts i, j represent the axial and radial direction, respectively. u_i are the axial and radial components of the blood velocities, $\widehat{u}_j$ represents the mesh velocity. $(u_j - \widehat{u}_j)$ is the relative velocity of the blood with respect to the moving coordinate velocity.

2.3. Wall modeling

The blood vessel wall is considered to be isotropic and elastic with Young's modulus E=0.7×10^6 *N/m*^{2}, Poisson's ratio ν=0.49 and density of blood vessel wall ρ_s=2000 *kg/m*^{3}. The thickness of the vessel wall is assumed to be uniform, t_h=1 *mm*, in normal region while the maximum thickness at the throat of the stenotic region is 2.5 *mm*.

The motion of an elastic vessel wall is mathematically described by the equation shown below:

$$\rho_s \frac{\partial^2 d_i}{\partial t^2} = \frac{\partial \sigma_{ij}}{\partial x_j} \tag{3}$$

where ρ_s is the vessel wall density, d_i are the components of the wall displacements and σ_{ij} are the components of the

wall stress tensor.

Under the assumption of an isotropic elastic material in which there is no change of temperature, Hooke's law may be stated in the form

$$\sigma'_{ij} = 2G\varepsilon'_{ij} \tag{4}$$

where σ'_{ij} and ε'_{ij} are the stress deviation and strain deviation, respectively;

$$\sigma'_{ij} = \sigma_{ij} - \frac{1}{3}\sigma_{\alpha\alpha}\delta_{ij} \tag{5}$$

$$\varepsilon'_{ij} = \varepsilon_{ij} - \frac{1}{3}\varepsilon_{\alpha\alpha}\delta_{ij} \tag{6}$$

where δ_{ij} is kronecker delta, $\frac{1}{3}\sigma_{\alpha\alpha}$ is the mean stress at a point and $\varepsilon_{\alpha\alpha}$ is the change of volume per unit volume. $\sigma_{\alpha\alpha}$ and $\varepsilon_{\alpha\alpha}$ are both invariants.

The stress tensor σ_{ij} can be obtained when we substitute Equations (5) and (6) into (4)

$$\sigma_{ij} = 2G\varepsilon_{ij} + \lambda\varepsilon_{kk}\delta_{ij} \tag{7}$$

$$G = \frac{E}{2(1+\nu)}, \quad \lambda = \frac{2G\nu}{1-2\nu} \tag{8}$$

λ and G are the first and second Lame parameters. The constant E is called the modulus of elasticity (Young's modulus) and the constant ν is called Poisson's ratio.

The conditions of displacement compatibility and traction equilibrium along the fluid-structure interface are satisfied:

· Displacement compatibility

$$\vec{d}_f = \vec{d}_s \tag{9}$$

· Traction equilibrium

$$\vec{f}_f = \vec{f}_s \tag{10}$$

where $\vec{d}$ and $\vec{f}$ are displacement and tractions and the subscripts f and s stand for fluid and solid respectively.

2.4. Boundary conditions and numerical method

The physiological flow at the inlet is specified by the temporal waveform given by Zendehbudi and Moayeri (1999) in the canine femoral artery as shown in Fig. 2. In this study the mean velocity, $\bar{U} = 0.33$ m/s, corresponding to $Re = 400$ is applied. The maximum velocity in Fig. 2 is 0.66 m/s. The inlet velocity initially accelerates and reaches a maximum at $t = 0.16$ (point A). After this point the velocity magnitude begins to decrease and drops to -0.185 m/s at $t = 0.42$ (point D). In this study the results can be compared at five different times corresponding to the conditions of accelerating point A, peak forward (point B), decelerating point (point C) and peak backward (point D and E) on each waveform.

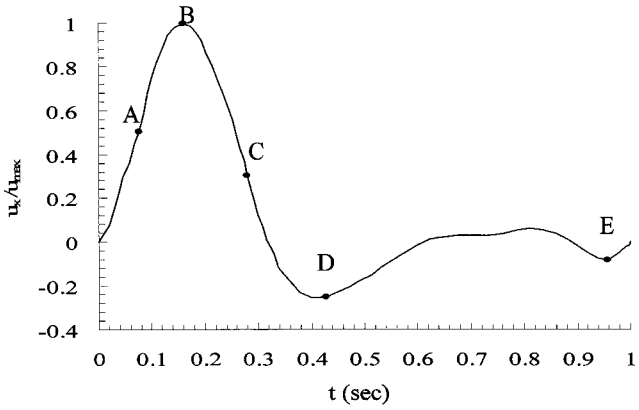

Fig. 2. Time variation of mean velocity for the physiological pulsatile flow (Zendehbudi and Moayeri, 1999).

No-slip conditions are imposed at the interfaces of the blood flow on the arterial wall. At the outlet, flow satisfies zero pressure flow conditions. On the axis of symmetry the axial velocity gradient and cross flow will be zero ($\frac{\partial u_x}{\partial r} = u_r = 0$ at $r = 0$).

The governing equations were solved using finite element commercial computational fluid dynamic software ADINA (version 8.4, ADINA, Watertown, MA) (Adina R&D, Inc., 2005). Fluid flow was solved by applying the direct solution method with applied 0.8 relaxing force and displacement. Meshing was composed of Rule-Based meshing method which is a Structural Meshing Algorithm. Simulation results were assumed to be independent of the computational mesh when the disparity between meshes of varying densities was less than 5%. The Newton method has been adopted as the iterative algorithm in all simulations. Maximum iteration repeated 15 times in order to in one step and allowable error was 10^{-5}. Time periodic solutions were typically obtained after 3 cycles and were defined when the cycle average difference in the size of the recirculation zone in the vicinity of the stenotic region fell below 5%.

All the computations were performed on an Intel Pentium IV 3.19 GHz with 3.5 GB RAM operating Windows XP. The computational solving process under the physiological inlet flow conditions took approximately 4 hours CPU time for No FSI model and several days CPU time for FSI model.

3. Results and discussion

3.1. Model validation

In order to validate the accuracy of the ADINA FSI solver at the beginning of computation, we were carried out the simulations for some of the typical cases considered by Lee and Xu (2002) and confirmed that we obtained similar results as shown in Fig. 3.

The numerical model of blood flow was carried out the

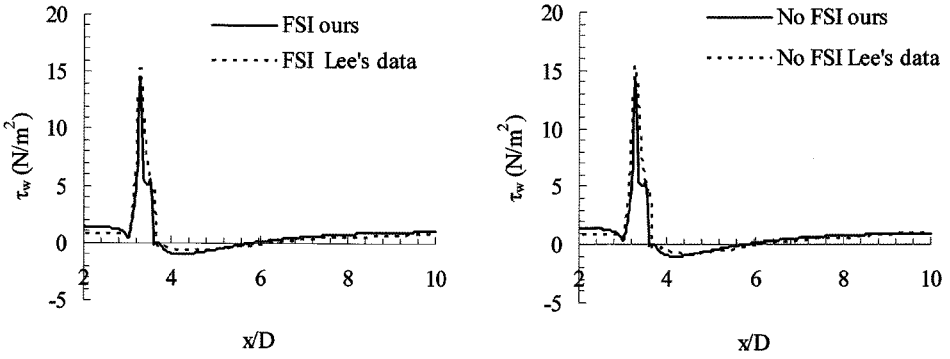

(a) Comparison of FSI cases (b) Comparison of No FSI cases

Fig. 3. Comparison of the wall shear stresses with our and results of Lee and Xu (2002).

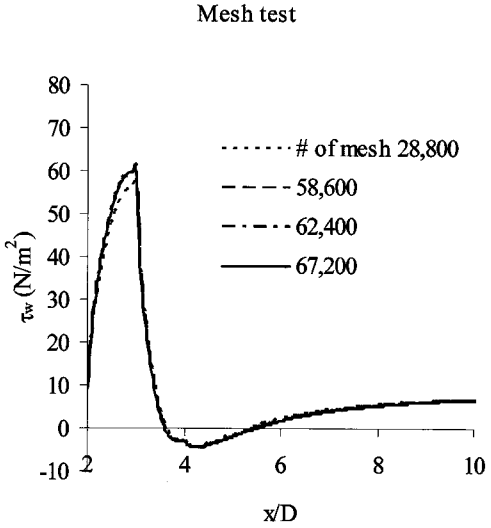

Fig. 4. The wall shear stresses along the vessel wall for 4 different numbers of meshes.

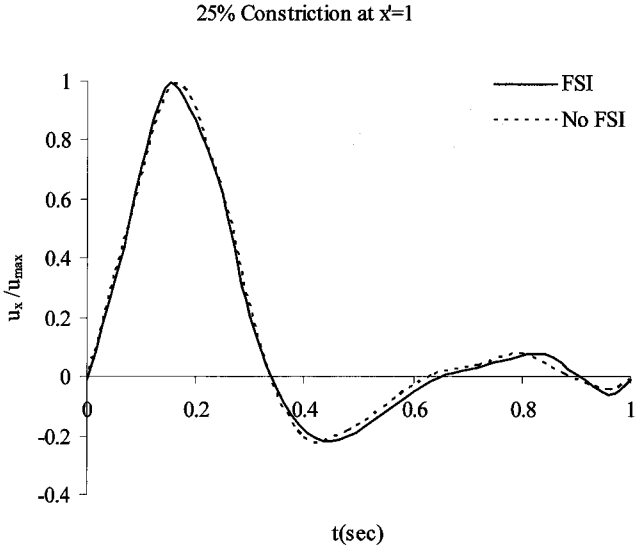

Fig. 5. Comparison of centerline axial velocity between FSI and No FSI models in the case of 25% stenosis at x'=1.

mesh independence test in Fig. 4 at the location x' (=x/D) =1, where x' is the normalized distance from the center of the stenosis. All simulations in this study were adopted the mesh in the range of 62,400 to 67,200.

3.2. Velocity field

Fig. 5 shows the comparison of the centerline velocities simulated for both No FSI and FSI models at the location x'=1 for 25% constriction of the cross-sectional area. The centerline axial velocity profile has the same pattern of the inlet physiological velocity waveform. During acceleration and early flow deceleration, there is small difference of the velocity profiles between two models. However, the differences between two models were found to be greater in the reversed flow period.

Fig. 6 shows the axial velocity profiles of the flow at five different times at the location x'=1 of 25%, 50% and 75% stenosis. As the flow rate with time is increased under the same stenosis rate, the peak velocity profile at the centerline is increased. The size of the flow separation indicated by negative velocity region near the wall also changed with time. The size of the recirculation region at point B of 75% stenosis case is approximately 1.4 times larger than at 50% stenosis one when compared Figs. 6(b) and 6(c).

3.3. Wall shear stress

Wall shear stress distributions along the axial direction presented at 5 different times in the cycle as shown in Fig. 7. Maximum wall shear stress occurred at point B at the throat of the stenosed region while minimum wall shear stress occurred at point D. Furthermore, point C indicates how the wall shear stress rapidly declined with time variation at 25%, 50% and 75% stenotic rates cases.

The magnitude of wall shear stress was largest at point B when flow was the maximum in the cycle. Peak wall shear stress is given at point B by the FSI model was 33.64 (N/m^2) at 25% stenosed rate case, in case of 50% case was

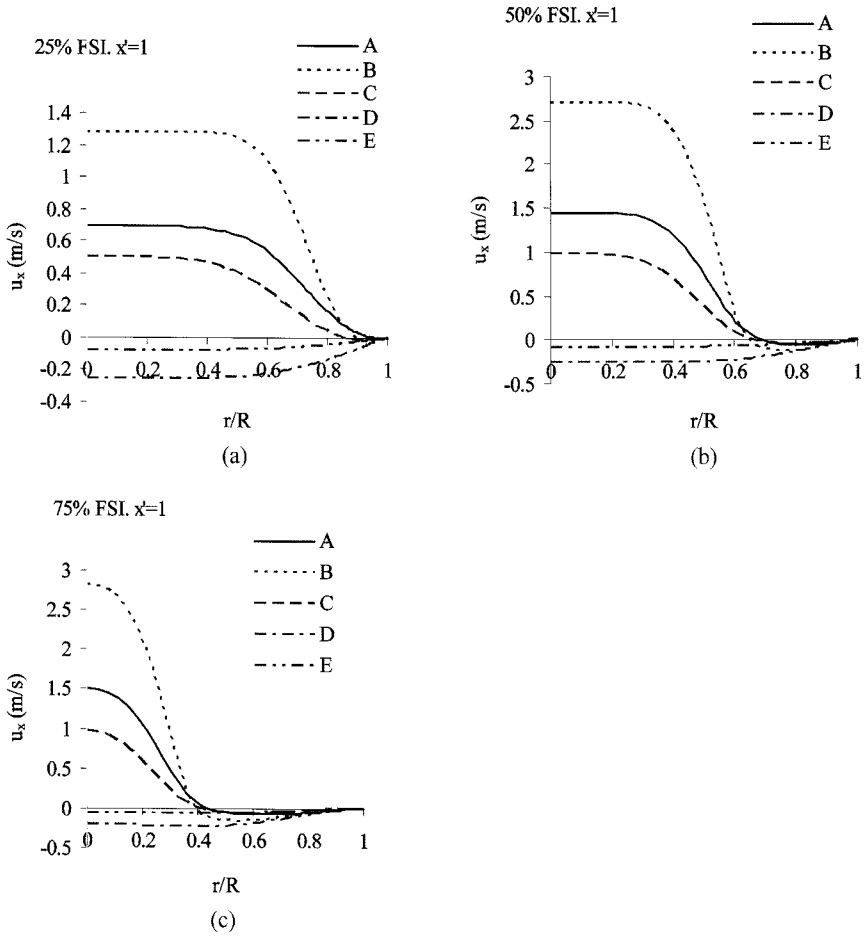

Fig. 6. Comparison of axial velocity profiles between the No FSI and FSI models at normalized post-stenotic distance of x'=1.

165.5 (N/m^2); 75% case was 167.78 (N/m^2), respectively.

Fig. 8 shows the pressure distribution along the blood vessel wall at 3 different stenosis rates. As we expected, the largest pressure drop is occurred at the time of peak flow (not shown as Figure). As the stenosis rate is increased, the pressure drop increases. The pressure drop is the largest when the stenosis rate is 75%. As shown in Fig. 8, the pressure drop is not sensitive when the stenosis rate is greater than 50%. The minimum pressure occurred just downstream of the stenosis as shown in Fig. 8.

According to the clinical point of view, shear stress is more essential. When blood force distribution acts on the boundary surfaces of stenosed area, high shear stress occurs at throat section of stenosed area and rapidly drops reversing its direction. If the stenosed rate increases, high shear stress occurs at the vicinity of the stenosed area which means that blood flow could be closure or vessel wall could collapse because of high stenosed rate and high shear stress (Fry, 1968; Ramstack *et al.*, 1979; Tang *et al.*, 2001b). Our results showed that the highest shear stress occurred at 50% and 75% stenosed ratios, which could cause shutting down of blood supply. Furthermore, according to the clinical trials, 20% is the average stenosis rate that subsequently ruptures with resulting complete artery closure.

3.4. Recirculation zone

Recirculation zones were carefully calculated by using negative wall shear stresses, in which occurred down side of stenosed region. Fig. 9 shows plotted recirculation zones with different percentage of stenosed rate cases. The smallest recirculation zones occurred at 25% stesosed rate case. Comparison among the stenosed rates described size of recirculation zone. When stenosis rate increased from 25% to 75% stenosed rate, recirculation zone gradually occurred longer and thicker. The most recirculation zone occurred at 75% stenosed rate case at the vicinity of the stenosed region. Moreover, Figs. 6 and 7 depict how recirculation registered near the wall when percentage of stenosed rate increased.

Medical research and studies suggest that recirculation is more essential in the cardiovascular system. Blood is circulated around the body through blood vessels by the pumping action of the heart. Therefore, normally blood flow condition regulates all blood hemodynamic factors

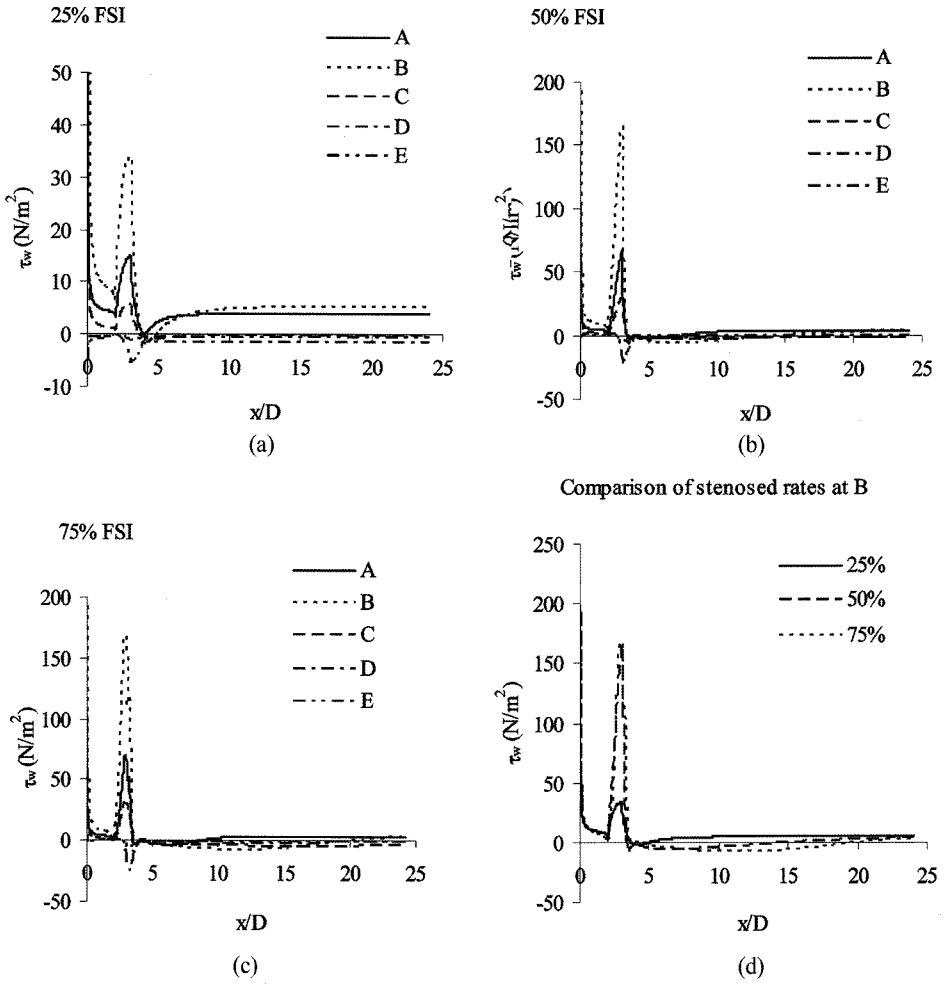

Fig. 7. Wall shear stress distributions with time variations at different stenosed rates.

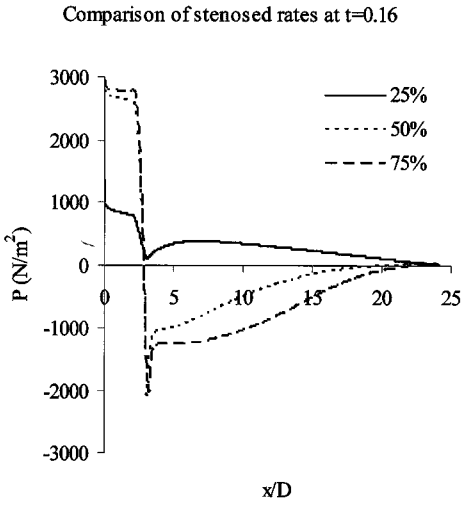

Fig. 8. Pressure distributions along the blood vessel wall at different stenosed rates.

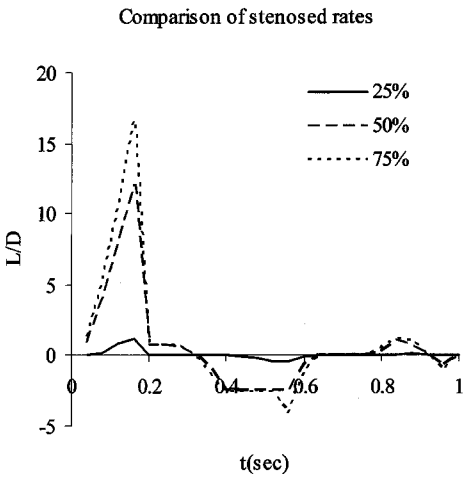

Fig. 9. Recirculation zone with time variation at different stenosed rates.

such as blood pressure, force, velocity, deformation, stress and others. Any change in regulation of blood flow would make the blood flow function unstable. In this connection, outcome of our simulation results showed that change of

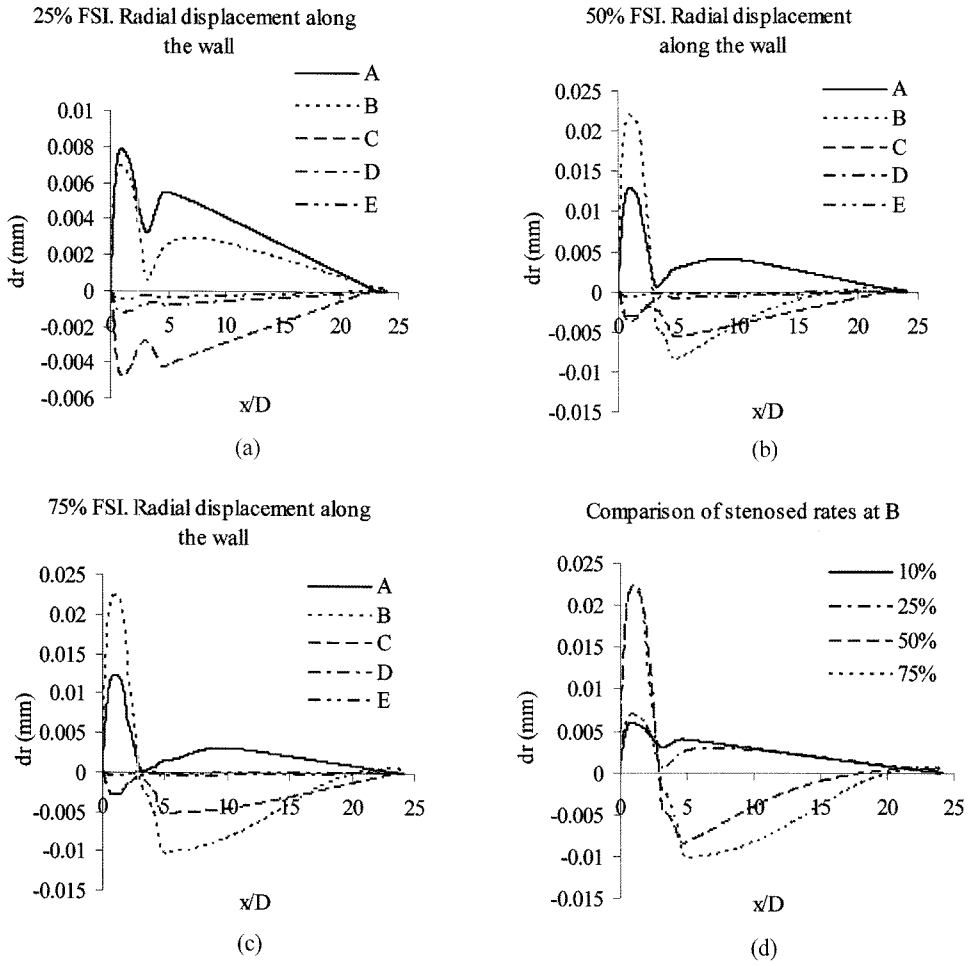

Fig. 10. Radial wall displacement distributions with time variation at various stenosed rate under the physiological condition.

blood flow condition over the throat section of 50% and 75% stenosed area could make blood flow abnormal due to recirculation zone. If recirculation zone occurs downstream of stenosed area, a fraction of the blood might remain on the downside of the area. Consequently, blood flow is interrupted resulting into abnormality in blood circulation.

3.5. Wall displacement

Fig. 10 shows radial wall displacements with time variation along the blood vessel. Inlet and outlet conditions were fixed at the solid part of FSI model by setting zero displacement. The wall model is constrained significantly for all the three stenosed rate cases. As shown in Fig. 10, the maximum radial wall displacement significantly stretched out at point B at the stenosed area while minimum radial wall displacement lengthened at point D in cases of 50% and 75% stenoted rate cases. However, the maximum stretch occurred at point A while minimum stretch occurred at time point D in cases of 10% and 25% stenoted rate cases.

Results of radial wall displacements were compared with all stenosed rate cases at time point B. Comparison results show that radial wall stretch was smallest at 10% stenosed rate case. In case of 50% and 75% cases, radial wall stretch was higher and longer, and these 2 cases can effect on blood artery, moreover, could collapse the artery (Fry, 1968).

4. Concluding remarks

In this study, we have used FSI to investigate the flow coupled with the solid structure at 25%, 50% and 75% stenosed rate cases by using commercial CFD code, ADINA 8.4 program. Of particular interest has been the impact of stenosis rates under the assumption of the physiological velocity profile. The potential role of the fluid mechanical phenomena may involve an effect of hemodynamic factors on the blood vessel collapse.

The fluid dynamic and vessel mechanical behavior were found to be an axisymmetric from the results for flow velocity and wall shear stress. In the axial velocity profiles of No FSI and FSI models were compared, and results of velocity profiles were very much same pattern for both models.

The effects of FSI models on the stenosis were small at 25% stenosed rate case and did not change the fluid and solid behavior significantly at 25% stenosed rate case. However, in case of 50% and 75% cases, the effects of FSI model on the stenosis were high which means blood flow could be closure or vessel wall could be collapsing due to high stenosed rate and high shear stress (Fry, 1968; Tang *et al.*, 2001b).

The wall shear stress rose sharply and declined quickly reversing its direction at the vicinity of the stenosed region as expected. The maximum wall shear stress occurred at point B (t=0.16) while the minimum wall shear stress occurred at point D (t=0.42) with time variation (Fig. 7).

Flow separation zones were observed in the post-stenotic downstream. Comparisons of x'=1 at point B show that when stenosed rate increased from 25% to 75%, reverse flow gradually increased and tended to be thicker and longer.

Comparison results of radial wall displacement show that radial wall displacement stretch was smallest at 10% stenosed rate case. In case of 50% and 75% cases, radial wall stretch was higher and longer, and these 2 cases could effect on blood artery.

Unsteady wall shear stress and of other hemodynamic variables were compared with experimental data by Lee and Xu (2002). Our computed results were compared with data of Lee and Xu (2002) to validate the numerical method and computer code. Comparisons results between ours and data of Lee and Xu (2002) indicated good agreement.

According to clinical point, hemodynamic factors play an important role on the localization of early atherosclerotic lesions. Our 50% and 75% stenosed rate cases could effect on blood artery due to hemodynamic factors. Fry (1968) said shear stresses may severely damage endothelial cells, or even strip them from the vessel.

References

ADINA R & D, Inc., 2005, Theory and modeling guide, Watermelon, MA.

Buchanan, Jr., J. R., C. Kleinstreuer and J. K. Comer, 2000, Rheological effects on pulsatile hemodynamic in a stenosed tube, *Computers & Fluids* **29**, 695-724.

Fry, D. L., 1968, Acute vascular endothelial changed associated with increased blood velocity gradients, *Circ. Res.* **22**, 165-197.

Glagov S., E. Weisenberg , C. K. Zarins, R. Stankunavicius and G. J. Kolettis, 1987, Compensatory enlargement of human atherosclerotic coronary arteries, *N. Engl. J. Med.* **316(22)**, 1371-1375.

Karino, T., T. Asakura and S. Mabuchi, 1988, Flow patterns and preferred sites of atherosclerosis in human coronary and celebral arteries, in 'Role of blood flow in atherosclerosis' (editor: Y. Yoshida, T. Yamaguchi, C. C. Caro, S. Glagov, and R. M. Nerem), Springer-Verlag.

Ku. D. N, C. K. Zarins, D. P. Giddens and S. Glagov., 1985, Early atherosclerosis and pulsatile flow in the human carotid bifurcation, *Arterioscler. Thromb, Vasc. Biol.* **5**, 293-302.

Lee. K. W and X. Y. Xu, 2002, Modelling of flow and wall behavior in a mildly stenosed tube, *Medical Engineering & Physics* **24**, 575-586

Powell B. E., 1991, Experimental measurements of flow through stenotic collapsible tubes, M. S. Thesis, Georgia Inst. of Tech.

Ramstack, J. M., Zuckerman, L. and Mockros, L. F., 1979, Shear induced activation of platelets, *J. Biomech.* **12**, 113-125.

Tang. D., C. Yang, S. Kobayashi and D. N. Ku, 2001a, Experiment – based numerical simulation of unsteady viscous flow in stenotic collapsible tubes, *Appl. Numer. Math.* **36(2-3)**, 299-320.

Tang D., C. Yang, S. Kobayashi and D. N. Ku, 2001b, Steady flow and wall compression in stenotic arteries: a three-dimensional thick-wall model with fluid-wall interactions, *J. Biomech. Eng.* **123(6)**, 548-557.

Yamaguchi, T., T. Kobayashi and H. Liu, 1998, Fluid – wall interactions in the collapse and ablation of an atheromatous plaque in coronary arteries, *Proc. Third World Congress of Biomechanics*, 20b.

Zendehbudi, G. R. and M. S. Moayeri, 1999, Comparison of physiological and simple pulsatile flows through stenosed arteries, *J. Biomech.* **32**, 959-965.